Biosensors and Bioelectronics 38 (2012) 284–288

Contents lists available at SciVerse ScienceDirect

Biosensors and Bioelectronics

journal homepage: www.elsevier.com/locate/bios

Chemiluminescence flow biosensor for glucose using Mg-Al carbonate layered double hydroxides as catalysts and buffer solutions

Zhihua Wang, Fang Liu, Chao Lu *

State Key Laboratory of Chemical Resource Engineering, Beijing University of Chemical Technology, Beijing 100029, China

ARTICLE INFO

Article history:
Received 9 May 2012
Accepted 1 June 2012
Available online 26 June 2012

Keywords:
Layered double hydroxides
Chemiluminescence
Glucose
Biosensor

ABSTRACT

In this work, serving as supports in immobilizing luminol reagent, catalysts of luminol chemiluminescence (CL), and buffer solutions for the CL reaction, Mg-Al-CO_3 layered double hydroxides (LDHs) were found to trigger luminol CL in weak acid solutions (pH 5.8). The silica sol–gel with glucose oxidase and horseradish peroxidase was immobilized in the first half of the inside surface of a clear quartz tube, and luminol-hybrid Mg-Al-CO_3 LDHs were packed in the second half. Therefore, a novel CL flow-through biosensor for glucose was constructed in weak acid solutions. The CL intensity was linear with glucose concentration in the range of 0.005–1.0 mM, and the detection limit for glucose (S/N=3) was 0.1 μM. The proposed biosensor exhibited excellent stability, high reproducibility and high selectivity for the determination of glucose and has been successfully applied to determine glucose in human plasma samples with satisfactory results. The success of this work has broken the bottleneck of the pH incompatibility between luminol CL and enzyme activity.

1. Introduction

Diabetes mellitus is a chronic disease characterized by high blood sugar (glucose) either because the body does not produce sufficient insulin, or cells do not respond to the produced insulin. It is a major and growing public health problem across the world. If diabetes is not adequately controlled, the patient has a significantly higher risk of developing complications, such as hypoglycemia, ketoacidosis, and metabolic disruption (Skyler, 2004). The International Diabetes Federation estimates that about 360 million people worldwide are living with diabetes, which is expected to rise to 552 million by 2030 if no urgent action is taken (Veerapur et al., 2012). Therefore, the determination of glucose is of importance in the monitoring of diabetic diets. The majority of conventional glucose sensors rely on an enzymatically based sensing scheme (Amerov et al., 2005; Hua et al., 2012; Li et al., 2010; Tierney et al., 2009).

In the past few years, chemiluminescence (CL) flow-through sensors have received increasing attention because of their operational convenience, instrumental simplification, environmental friendliness, low cost, resource savings and increased accuracy (Li et al., 2001; Yu et al., 2010; Zhou et al., 2005). The luminol CL reaction usually occurs in a strongly basic medium (pH 10–11); while glucose oxidase (GOD) retains its maximum activity at pH 5.5. Therefore, the known and well assessed luminol CL flow-through glucose sensors are generally fabricated by immobilizing GOD for the formation of H_2O_2 accompanying mobile luminol (Lan et al., 2008; Li et al., 2008; Lin et al., 2001). Due to the pH incompatibility issues, it is still a great challenge to achieve a micro-fabricated device immobilizing luminol and enzyme in one column.

Layered double hydroxides (LDHs) are an important class of host–guest materials consisting of positively charged metal hydroxide sheets with charge-balancing intercalated anions and water molecules (Bastianini et al., 2012; Evans and Duan, 2006). Mg-Al-CO_3 LDHs are extensively studied as actual catalysts, catalyst precursors, catalyst supports and optical materials due to their high stability and convenient synthesis (Chitrakar et al., 2011; Shi and He, 2011; Xu et al., 2010). Recently, we observed that Mg-Al-CO_3 LDHs can greatly catalyze the luminol–H_2O_2 CL reaction, and the CL intensity was in proportion to the concentration of Mg-Al-CO_3 LDHs; however, higher concentrations of Mg-Al-CO_3 LDHs were able to clog the tubing, which is becoming a significant limiting factor in their further applications (Wang et al., 2011a, 2011b).

In this study, the silica sol–gel with GOD and horseradish peroxidase (HRP) was immobilized in the first half of the inside surface of a clear quartz tube, and the luminol-hybrid Mg-Al-CO_3 LDHs were packed in the second half, which was constructed a CL flow cell, adjacent to a photomutiplier tube (PMT). In this case, Mg-Al-CO_3 LDHs served as supports in immobilizing luminol

* Corresponding author. Tel.: +86 10 64411957; fax: +86 10 64411957.
E-mail addresses: luchao@mail.buct.edu.cn, luchao20022002@yahoo.com.cn (C. Lu).

0956-5663/$ - see front matter © 2012 Elsevier B.V. All rights reserved.
http://dx.doi.org/10.1016/j.bios.2012.06.003

reagent, catalysts of luminol chemiluminescence (CL), and buffer solutions for the CL reaction (Cheng et al., 2009; Mandal et al., 2009; You et al., 2001). Therefore, using this simple micro-fabricated device, a stronger light can also emit in weak acid or neutral medium. This novel CL flow-through biosensor has been successfully applied to determine glucose in human plasma samples with simple procedures, shorter response time, high selectivity and wide pH compatibility.

2. Experimental

2.1. Chemicals and solutions

Analytical grade chemicals including $Mg(NO_3)_2 \cdot 6H_2O$, $Al(NO_3)_3 \cdot 9H_2O$, Na_2CO_3, glucose and NaOH were purchased from Beijing Chemical Reagent Company, and were used without further purification. A 0.01 M stock solution of luminol (3-aminophthalhydrazide) was prepared by dissolving luminol (Acros, USA) in 0.1 M NaOH solution without purification, and was used after about two weeks in order to make the luminol solution stable. GOD (from *Aspergillus niger*, $\geq$264 U/mg) and HRP (1000 U/mg) were obtained from SERVA Electrophoresis GmbH (Germany). The GOD solution was prepared by dissolving 5.4 mg GOD in 1.0 mL phosphate buffer (pH 7.4) and the HRP solution was prepared by dissolving 10.8 mg HRP in 1.0 mL phosphate buffer (pH 7.4). Glucose stock solution was prepared with deionized water and stored for at least 48 h before use to allow mutarotation to take place. Working solutions of H_2O_2 were prepared daily from 30% (v/v) H_2O_2 (Beijing Chemical Reagent Company, China). All solutions were prepared with deionized water (Milli Q, Millipore, Barnstead, CA, USA).

2.2. Apparatus

The powder X-ray diffraction (XRD) measurements were performed on a Bruck (Germany) D8 Advance X-ray diffractometer equipped with graphite-monochromatized Cu/Kα radiation (λ=1.54178 Å). The 2θ angle of the diffractometer was collected in the range from 5° to 75°. The Raman spectra were collected by a Renishaw Micro-Raman Spectroscopy InVia Raman system (England). A Renishaw red laser excitation at 785 nm was employed as the excitation source. Hitachi (Japan) S-4700 field-emission scanning electron microscope (SEM) was used for obtaining the scanning electron microscopy images. The CL spectra were obtained using a F-7000 fluorescence spectrophotometer (Hitachi, Japan) at a slit of 10.0 nm with a scanning rate of 1200 nm/min. UV–vis spectra were measured on a USB 4000 miniature fiber optic spectrometer in absorbance mode with a DH-2000 deuterium and tungsten halogen light source (Ocean Optics, Dunedin, FL). The CL detection was conducted on a BPCL luminescence analyzer (Institute of Biophysics, Chinese Academy of Science, Beijing, China).

2.3. Procedures

2.3.1. Synthesis of Mg-Al-CO_3 LDHs

Mg-Al-CO_3 LDHs were prepared by the coprecipitation method at constant pH under low supersaturation conditions. $Mg(NO_3)_2 \cdot 6H_2O$ (0.045 mol) and $Al(NO_3)_3 \cdot 9H_2O$ (0.015 mol) were dissolved in 60 mL deionized water. The pH of the solution remained 10 by drop-wise addition of 60 mL alkali liquor (0.12 mol NaOH and 0.0075 mol Na_2CO_3). The resulting slurry was aged for 24 h at 60 °C. The product was centrifuged and washed with deionized water 3–4 times and dried at 60 °C for 24 h. Then the slurry was dried for 24 h at 60 °C. The as-prepared Mg-Al-CO_3 LDHs were grinded and passed through a standard sieve to get the size from 0.45 to 0.80 mm.

2.3.2. Preparation of luminol-hybrid LDHs

To prepare luminol-immobilized sensor, 0.20 g Mg-Al-CO_3 LDHs were packed into a quartz tube (5 cm in length and 0.6 cm i.d.) and furnished with glass wool at both ends to prevent the loss of Mg-Al-CO_3 LDHs. 0.01 M luminol solution was pumped into the column at 1.0 mL/min for 15 min. The as-prepared column was washed with deionized water until the baseline kept steady. Finally, the light yellow luminol-immobilized column was obtained (Fig. 1).

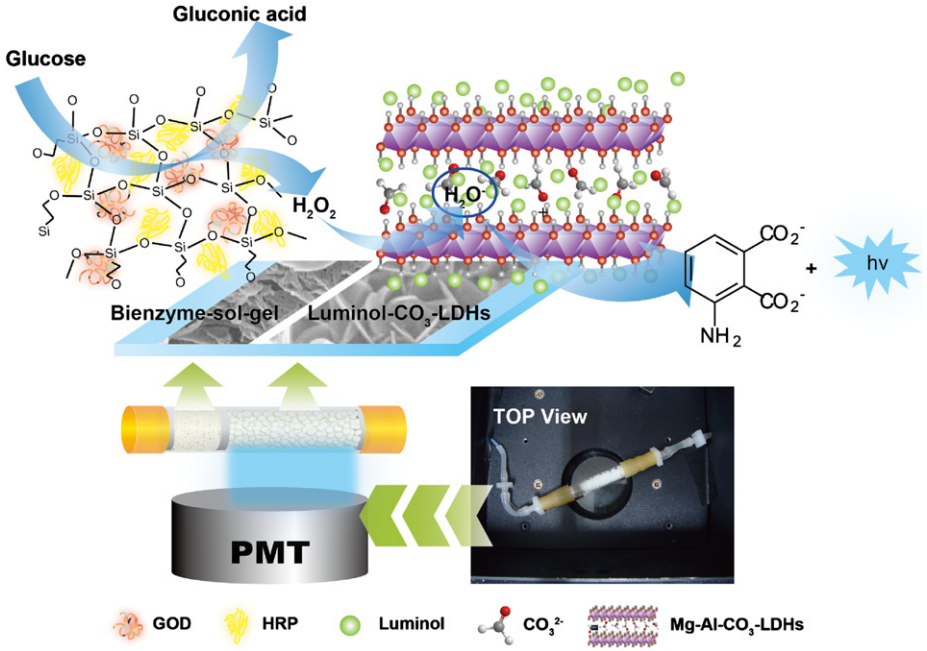

Fig. 1. Schematic illustration of platform fabricated by bienzyme and luminol-hybrid Mg-Al-CO_3 LDHs. Top: illustration of the experimental procedure of the biosensor for glucose. Left down: scheme of the CL flow-through biosensing device. Right down: photo of the CL flow-through biosensing device.

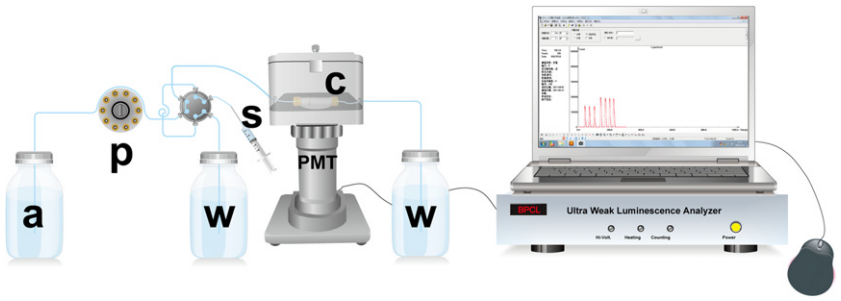

Fig. 2. Schematic diagram of the CL flow-through biosensor for glucose. a, H_2O at 2.1 mL/min; s, sample (150 μL); c, column (5 cm in length and 0.6 cm i.d.); w, waste; p, peristaltic pump; PMT, photomultiplier tube (−1000 V).

2.3.3. *Immobilization of bienzyme*

A transparent sol–gel stock solution was obtained by mixing 2.2 mL TEOS, 0.7 mL H_2O and 50 μL HCl (0.1 mol/L) in a glass vial with stirring for 3 h. The as-prepared sol–gel solution was stored in a refrigerator at 4 °C. The mixed solution of 30 μL GOD and 30 μL HRP was added into 0.4 mL sol–gel stock solution. By a spreading method, the mixture was coated on the interior surface of a quartz tube, and then was allowed to polymerize for about 40 min and become a gel at room temperature. Therefore, the sol–gel was stuck tenaciously to the inner surface of the quartz tube to form a glucose-sensitive matrix. In order to prevent the glucose-sensitive matrix cracking as a result of rapid evaporation, both ends of the quartz tube were sealed during the gels aging. The storage after gelation was carried out at 4 °C (see Fig. 1).

2.3.4. *CL measurements*

The schematic diagram of the flow injection analysis (FIA) was illustrated in Fig. 2. It consisted of one peristaltic pump (BT-100M, Baoding, China), a 150 μL loop injector, six-way injection valve (Shimadzu, Tokyo, Japan), a quartz tube, and a BPCL luminescence analyzer. The flow rate for the carrier stream was 2.1 mL/min. 150 μL glucose solution was injected into water carrier stream by a loop valve injector. Afterwards, glucose standard or sample solution flowed through the column, which was placed in front of PMT. The CL signals were monitored by PMT adjacent to the CL flow-through biosensor. The signals were imported to the computer for data acquisition.

3. Results and discussion

3.1. *Adsorption of luminol on the surface of Mg-Al-CO_3 LDHs*

Positively charged LDHs are able to absorb anionic species from aqueous systems by surface adsorption, ion-exchange/intercalation, and reconstruction. The surface adsorption involves the adhesion of anionic species to the surface of LDHs, thus allowing the formation of a molecular or atomic film (Chuang et al., 2008; Zhou et al., 2011). CO_3 anions have very strong affinity for LDH layers, and thus other anionic species can only adhere well to the surface of Mg-Al-CO_3 LDHs by surface adsorption (Sharma et al., 2008). Fig. 3 showed the powder XRD patterns of the synthesized Mg-Al-CO_3 LDHs before and after surface-adsorbed luminol. The sharp and symmetric reflections for (003), (006), (110) and (113) planes characteristic of Mg-Al-CO_3 LDHs indicated the typical and well-order layered structures with a high degree of crystallinity before and after surface-adsorbed luminol (Batistella et al., 2011). Moreover, as shown in Fig. S1, the Raman peaks at 548 and 1050 cm^{-1} were corresponding to the ring skeletal vibration and C–N stretch of luminol (Premasiri et al., 2005; Yin et al., 2011). These phenomena demonstrated that luminol dianions were

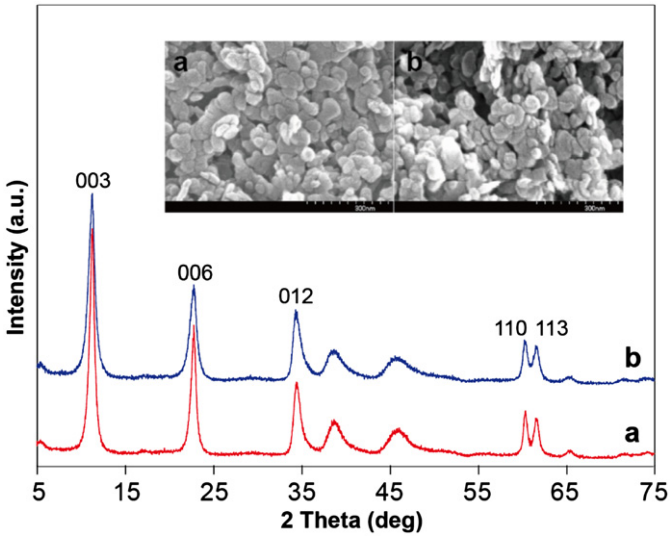

Fig. 3. Powder XRD patterns and SEM images of Mg-Al-CO_3 LDHs (a) before and (b) after surface adsorbed luminol. For XRD patterns, the 2θ angle of the diffractometer was stepped from 5° to 75° at a scan rate of 0.02°/s. For SEM images, the as-prepared Mg-Al-CO_3 LDHs colloidal solution was dropped on glass substrate.

sufficiently absorbed on the surface of Mg-Al-CO_3 LDHs. Next, the effect of the adsorbed amounts of luminol on the CL intensity was investigated (Fig. S2). We can see that the CL intensity increased with increasing the adsorbed amount of luminol in the range of 0.05–0.15 mmol; however, the concentrations of luminol higher than 0.15 mmol caused a slight CL decrease, which might be attributed to the absorption of the emitted light for the light yellow color of the excess of luminol.

3.2. *Buffering capacity of Mg-Al-CO_3 LDHs*

The relationship between the initial and equilibrium pH was presented in Fig. 4a. It was interesting to observe that the equilibrium pH of the solution remained almost constant (pH 9.0) upon increasing the initial pH from 4.0 to 10.0. However, the equilibrium pH decreased sharply on either further lowering the initial pH toward strongly acidic media or further increasing the initial pH toward highly alkaline media. The strong buffering capacity of the LDHs may be due to partial dissolution of the LDHs in acidic media or the adsorption of OH^- ions on the surface of the LDHs in alkaline media (Cheng et al., 2009; Mandal et al., 2009; You et al., 2001). In this study, we investigated the influence of the carrier pH in the range of 4.0–12.0 on the CL intensity of luminol-hybrid LDHs column by FIA technique. As shown in Fig. 4b, the CL intensity was not considerably affected in the pH range from 4.0 to 6.0. However, the CL intensity

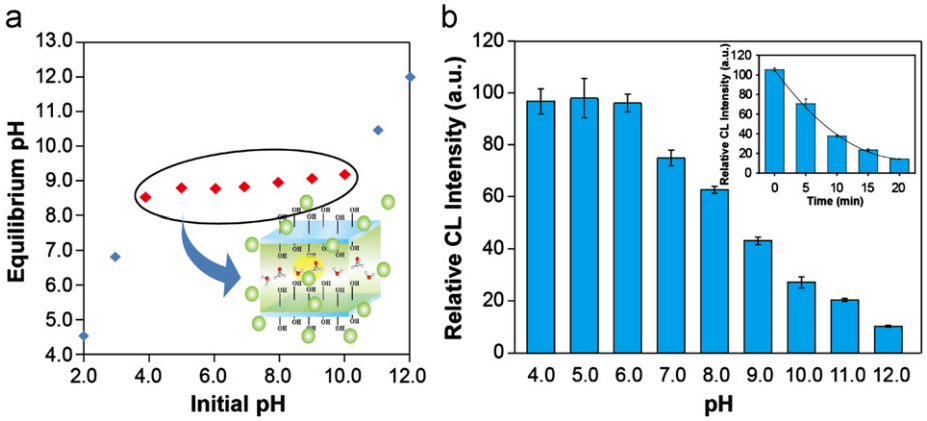

Fig. 4. (a) The pH buffering capacity of Mg-Al-CO_3 LDHs. The pH of the solution (25 mL) was adjusted with 1.0 M HCl or 1.0 M NaOH, and then 50 mg Mg-Al-CO_3 LDHs were added into the different pH solutions with continuous stirring for 30 min before the equilibrium pH of the solution was measured. (b) The influence of the pH in the carrier on the CL intensity of luminol-hybrid LDHs column. Inset: the effect of the elution time of the carrier (pH 12.0) on the CL intensity. The pH of the carrier was adjusted with 1.0 M HCl or 1.0 M NaOH.

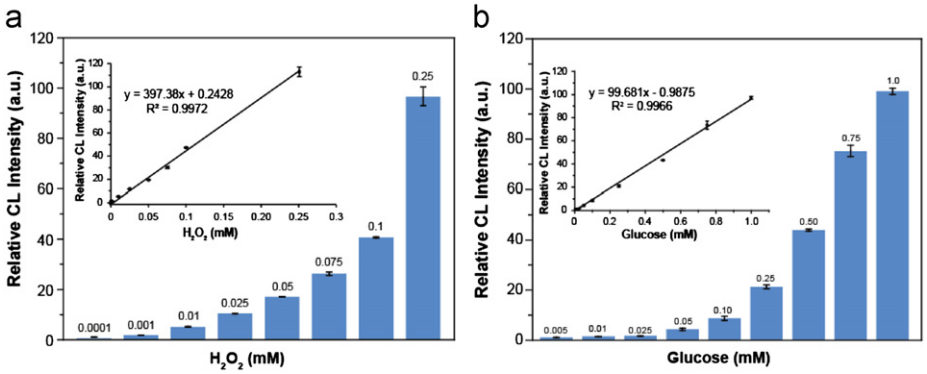

Fig. 5. CL intensity of the flow-through biosensor by adding different concentrations of H_2O_2 (a) and glucose (b). Inset: the calibration curves for H_2O_2 and glucose. The experimental conditions were the same as those described in the legend to Fig. 2.

decreased when the pH values in the carrier were above 6, which was probably due to the competitive adsorption between the increased OH^- ions and luminol dianions (inset of Fig. 4b).

3.3. Emitting species

The CL spectra of the luminol-hybrid LDHs column in the presence/absence of glucose were measured using a FL-7000 model spectrofluorimeter combined with a FIA system. As shown in Fig. S3, the maximum emission for the present system was about 455 nm. However, the maximum emission wavelength of luminol in basic conditions was usually about 425 nm. It was reported that the maximum fluorescent wavelengths of 3-aminophthalate anions in basic solutions (pH 10.5) and acidic solutions (pH 5.8) were 422 and 454 nm, respectively (Lin et al., 2001). Therefore, it is certain that the emitter of the present system is still the excited-state 3-aminophthalate anions, the same as those in the usual luminol CL reaction in basic solutions. These results demonstrated that the adsorbed luminol onto the surface of Mg-Al-CO_3 LDHs cannot generate a new luminophor.

3.4. Ratio of HRP to GOD

In order to maximize the yield of H_2O_2 produced from the enzyme-catalyzed oxidation of glucose as soon as possible, the bienzyme, HRP and GOD with a volume ratio of 1:1 (Fig. S4) was co-immobilized on the sol–gel matrix. The characteristics of GOD–HRP–sol–gel were evaluated using UV–visible spectra and SEM images (see Fig. S5). The peaks at about 280 and 400 nm were corresponding to amino acid residues in proteins and heme group of HRP, respectively (Marcos et al., 1999; Sanz et al., 2005). These results indicated that the secondary structures of GOD and HRP were maintained after they were encapsulated in the sol–gel, which was necessary to keep the native activity of enzymes. Moreover, the morphologies of sol–gel and bienzyme–sol–gel displayed a chemically clean three-dimensional uniform porous structure, and the sol–gel matrix produced a narrower particle size distribution, facilitating the bienzyme loading (inset of Fig. S5).

3.5. Performances of biosensor for glucose sensing

The analytical performances of the proposed method were examined under the optimum conditions. The calibration curves were found to be linear from 0.0001 to 0.25 mM for H_2O_2 (Fig. 5a) with a regression line $y=397.38x+0.2428$ ($R^2=0.9972$), 0.005 to 1.0 mM for glucose (Fig. 5b) with a regression line $y=99.681x-0.9875$ ($R^2=0.9966$), where y is CL intensity and x is the concentration of H_2O_2 or glucose, respectively. The detection limit for glucose (S/N=3) was 0.1 μM. Although the sensitivity of the proposed method was the same as those of the known and well assessed glucose CL sensors (Lan et al., 2008; Li et al., 2008; Lin et al., 2001), its selectivity was high enough because the luminol CL reaction of the present system can take place at quasi-neutral and slightly acidic pH. Moreover, our innovative approach was adequate for the levels of glucose allowable in human plasma samples. To assess the selectivity of the developed method, the

Table 1
Assay results of glucose in human plasma samples.

Samples	Standard method (mM)	Present method (mM)	Added (mM)	Found (mM)	Recovery (%)
Plasma 1	7.5 ± 0.2	7.1 ± 0.2	0.1	0.1 ± 0.002	96 ± 1.6
			0.2	0.2 ± 0.003	102 ± 1.5
Plasma 2	5.3 ± 0.1	5.6 ± 0.2	0.1	0.1 ± 0.0001	102 ± 0.1
			0.2	0.2 ± 0.0002	97 ± 0.1

All of the results were the mean of three determinations $\pm$S.D.

effects of typical commonly interferences present in human plasma samples were investigated (Table S1). A high selectivity of the proposed biosensor may be ascribed to the luminol CL emission of the present system in weak acid solutions.

The operational stability of this biosensor was investigated by 200 repeated measurements of 5.0 μM mM glucose, and the relative standard deviation was 2.8% (Fig. S6). On the other hand, the lifetime of this biosensor was examined by periodically checking its CL intensity. It was found that the CL intensity was approximately 95% of its initial value after two months.

3.6. Real samples

In order to evaluate the applicability and reliability of the proposed methodology, it was applied for the determination of glucose in real samples. Human plasma samples from some volunteers were collected from China–Japan Friendship Hospital (Beijing, China). Before detection, the samples were diluted 100 times by deionized water to yield testing sample solutions. The concentrations of glucose in human plasma samples were obtained using a standard addition method, and the results were in good agreement with those obtained by the dintro (DNS) method (Table 1) (López and Cavaco-Paulo, 2008). The accuracy of our method was tested by determining the recovery of known amounts of glucose added to the real samples. The good recovery values range from 96% to 102% indicated good accuracy of the proposed method. These satisfactory results demonstrated that the novel CL flow-through biosensor was reliable and effective.

4. Conclusions

This work has developed a novel CL flow-through biosensor for glucose on platform fabricated by bienzyme network and luminol-hybrid LDHs. In this case, the specific advantages of Mg-Al-CO_3 LDHs included the high buffering capacity and strongly catalyzing activity on the luminol CL, and thus a stronger light of the present system can emit in weak acid solutions by successfully immobilizing luminol and bienzyme in one column. The proposed CL flow-through biosensor showed excellent stability, high reproducibility, simple procedures and high selectivity for glucose, which has very large potential in the assays of other analytes by tuning enzyme species. Moreover, the improved selectivity for glucose will open new avenues not only for biochemical assays but also for environmental applications devoted to the monitoring of trace levels of H_2O_2 in water samples.

Acknowledgments

This work was supported by the National Natural Science Foundation of China (21077008, 20935002 and 20975010), the Program for New Century Excellent Talents in University (NCET-11-0561) and the Fundamental Research Funds for the Central Universities (ZZ1230).

Appendix A. Supporting information

Supplementary data associated with this article can be found in the online version at http://dx.doi.org/10.1016/j.bios.2012.06.003.

References

Amerov, A.K., Chen, J., Small, G.W., Arnold, M.A., 2005. Analytical Chemistry 77, 4587–4594.
Bastianini, M., Costenaro, D., Bisio, C., Marchese, L., Costantino, U., Vivani, R., Nocchetti, M., 2012. Inorganic Chemistry 51, 2560–2568.
Batistella, L., Venquiaruto, L.D., Luccio, M.D., Oliveira, J.V., Pergher, S.B.C., Mazutti, M.A., Oliveira, D.D., Mossi, A.J., Treichel, H., Dallago, R., 2011. Industrial & Engineering Chemistry Research 50, 6871–6876.
Cheng, X., Huang, X.R., Wang, X.Z., Zhao, B.Q., Chen, A.Y., Sun, D.Z., 2009. Journal of Hazardous Materials 169, 958–964.
Chitrakar, R., Sonoda, A., Makita, Y., Hirotsu, T., 2011. Industrial & Engineering Chemistry Research 50, 9280–9285.
Chuang, Y.H., Tzou, Y.M., Wang, M.K., Liu, C.H., Chiang, P.N., 2008. Industrial & Engineering Chemistry Research 47, 3813–3819.
Evans, D.G., Duan, X., 2006. Chemical Communications, 485–496.
Hua, M.-Y., Lin, Y.-C., Tsai, R.-Y., Chen, H.-C., 2012. Journal of Materials Chemistry 22, 2566–2574.
Lan, D., Li, B.X., Zhang, Z.J., 2008. Biosensors and Bioelectronics 24, 934–938.
Li, B.X., Lan, D., Zhang, Z.J., 2008. Analytical Biochemistry 374, 64–70.
Li, B.X., Zhang, Z.J., Jin, Y., 2001. Analytical Chemistry 73, 1203–1206.
Li, W.J., Yuan, R., Chai, Y.Q., 2010. Journal of Physical Chemistry C 114, 21397–21404.
Lin, J.-M., Shan, X.Q., Hanaoka, S., Yamada, M., 2001. Analytical Chemistry 73, 5043–5051.
López, C., Cavaco-Paulo, A., 2008. Engineering in Life Sciences 8, 315–323.
Mandal, S., Mayadevi, S., Kulkarni, B.D., 2009. Industrial & Engineering Chemistry Research 48, 7893–7898.
Marcos, S.D., Galindo, J., Sierra, J.F., Galbán, J., Castillo, J.R., 1999. Sensors and Actuators B 57, 227–232.
Premasiri, W.R., Moir, D.T., Klempner, M.S., Krieger, N., Jone II, G., Ziegler, L.D., 2005. Journal of Physical Chemistry B 109, 312–320.
Sanz, V., Marcos, S.D., Castillo, J.R., Galbán, J., 2005. Journal of the American Chemical Society 127, 1038–1048.
Sharma, U., Tyagi, B., Jasra, R.V., 2008. Industrial & Engineering Chemistry Research 47, 9588–9595.
Shi, H.M., He, J., 2011. Journal of Catalysis 279, 155–162.
Skyler, J.S., 2004. Journal of Medicinal Chemistry 47, 4113–4117.
Tierney, S., Hasle Falch, B.M., Hjelme, D.R., Stokke, B.T., 2009. Analytical Chemistry 81, 3630–3636.
Veerapur, V.P., Prabhakar, K.R., Thippeswamy, B.S., Bansal, P., Srinivasan, K.K., Unnikrishnan, M.K., 2012. Food Chemistry 132, 186–193.
Wang, Z.H., Liu, F., Lu, C., 2011a. Chemical Communications 47, 5479–5481.
Wang, Z.H., Liu, F., Teng, X., Zhao, C.X., Lu, C., 2011b. Analyst 136, 4986–4990.
Xu, Y.F., Dai, Y.C., Zhou, J.Z., Xu, Z.P., Qian, G.R., Max Lu, G.Q., 2010. Journal of Materials Chemistry 20, 4684–4691.
Yin, J., Wu, T., Song, J.B., Zhang, Q., Liu, S.Y., Xu, R., Duan, H.W., 2011. Chemistry of Materials 23, 4756–4764.
You, Y.W., Vance, G.F., Zhao, H.T., 2001. Applied Clay Science 20, 13–25.
Yu, J.H., Ge, L., Dai, P., Ge, S.G., Liu, S.Q., 2010. Biosensors and Bioelectronics 25, 2065–2070.
Zhou, H.J., Zhang, Z.J., He, D.Y., Xiong, Y., 2005. Sensors and Actuators B 107, 798–804.
Zhou, J.Z., Xu, Z.P., Qiao, S.Z., Liu, Q., Xu, Y.F., Qian, G.R., 2011. Journal of Hazardous Materials 189, 586–594.